

# **LINKED PHARMACODYNAMIC MODELS: DIFFUSION INTO ENDOCARDIAL VEGETATIONS, POSTANTIBIOTIC EFFECT, AND BACTERIAL GROWTH AND KILL**

Jelliffe R<sup>1</sup>, Barbaut X<sup>2</sup>, Maire P<sup>2</sup>, El Brouzi A<sup>3</sup>, and Vergnaud JM<sup>3</sup>.

1 - USC School of Medicine, Los Angeles, USA, 2 - ADCAPT, Hospices Civils de Lyon, France, and 3 - Faculty of Sciences, St. Etienne, France.

In this paper we will describe the linkage of nonlinear dynamic models to the basic linear pharmacokinetic model, and show some applications in cvlinical software describing drug diffusion into endocardial vegetations, the simulation of a postantibiotic effect, and the modeling of bacterial growth in the absence of a drug and its kill by an antibiotic.

## **MODELING DRUG DIFFUSION**

A problem in the treatment of patients with infectious endocarditis is that it is difficult to estimate if the drug is able to kill the organisms all the way into the center of a vegetation. Because of this, a diffusion model was made of this process.

A spherical shape was assumed for the vegetation, as shown in Figure 1, and it was modeled having several concentric layers, with diffusion taking place from layer to layer. The sphere was assumed to be homogeneous, with equal diffusion in all directions, and as having a constant coefficient of diffusion throughout. The diffusion was assumed to be dependent on the concentration of drug in the surrounding medium, such as the serum concentration, and its time course. The diameter of endocardial vegetations can be measured by transesophageal echocardiography.

The following equation was used to model the diffusion:

$$\frac{\partial C}{\partial t} = \frac{1}{r^2} \cdot \frac{\partial}{\partial r} [D \cdot r^2 \cdot \frac{\partial C}{\partial r}]$$

where C represents the concentration in the sphere at time t, at a distance r from the center of the sphere, and D represents the coefficient of diffusion in the sphere.

When D is assumed constant, the equation becomes

$$\frac{\partial C}{\partial t} = D \cdot \left[ \frac{\partial^2 C}{\partial r^2} + \frac{2}{r} \cdot \frac{\partial C}{\partial r} \right]$$

The vegetation is assumed to be continuously immersed in the surrounding medium, and the drug concentration in that medium is assumed to attain a value which results in equilibrium with the very outer layer of the sphere. The medium then undergoes the changes in concentration with time that constitute the serum level time course. This time course is thus presented as the input to the spherical model [1].

The diffusion coefficient found by Bayer, Crowell, et al. for aminoglycosides in experimental endocarditis [2,3] was used. The model has become part of the USC\*PACK clinical programs for individualizing drug dosage regimens [4]. The model can also be used to simulate behavior inside an abscess, and, by appropriate choice of sphere diameter and diffusion coefficient, to simulate the post-antibiotic effect of a certain desired duration.

### **Examples: Simulated Endocardial Vegetations of Various Diameters**

Suppose one were to develop an amikacin dosage regimen for a hypothetical 65 year old man, 70 in tall, weighing 70 kg, with a serum creatinine of 1.0 mg/dL. Let us assume that he has a vegetation seen by echocardiography on his aortic valve that might be either 0.5, 1.0, or 2.0 cm in diameter. We wish to examine the ability of an amikacin regimen designed to achieve serum peaks of 45 ug/ml and troughs of approximately 5.0 ug/ml to reach effective concentrations within the vegetation in these three cases. Let us apply the findings of Bayer et al [2,3] to compute the time course of probable amikacin concentrations in the center of these three vegetations of different

diameters, to examine their possible ability to kill an organism having an estimated minimum inhibitory concentration (MIC) of 8.0 ug/ml, for example.

Using the Amikacin program in the USC\*PACK collection [4], let us estimate, from the patient's age, gender, height, weight, and serum creatinine concentration, that his creatinine clearance (CCr) is about 69 ml/min/1.73M<sup>2</sup>. This method of estimating CCr is discussed in detail in another paper in this issue. We enter the target goal for the peak serum concentration of 45 ug/ml and an initial trough concentration of about 5.0 ug/ml. The ideal dose interval to achieve that peak and trough exactly, adjusted for the patient's renal function, employing a planned duration of the IV infusion of 0.5 hr, turns out to be 10.231 hrs. Let us approximate this in a practical manner by choosing a dose interval of 12 hrs. The dosage regimen to achieve the peak goal with such a dose interval is, when revised to practical amounts, 850 mg for the first dose, followed by 750 mg every 12 hrs thereafter.

On this regimen, predicted serum concentrations are 43 ug/ml for the peak and 3.2 ug/ml for the trough. The peak is 542 % of the stated MIC, and serum concentrations are predicted to be at least the MIC for 66 % of each dose interval. The AUC/MIC ratio for the first 24 hours is 48.8. The plot of these predicted serum concentrations is shown in Figure 2.

The important question now is whether or not this predicted serum concentration profile will result in adequate penetration of the vegetation in each of the three cases, and whether or not the regimen will kill effectively there, as well as in the central (serum level) compartment.

Figure 3 shows the predicted amikacin concentrations in the center of the simulated vegetation having a diameter of 0.5 cm. As shown, concentrations rise rapidly above the MIC and stay there, suggesting that the above regimen should probably be able to kill organisms having an MIC of about 8.0 ug/ml fairly promptly in the center of the vegetation. The time lag of concentrations in the center of the sphere is modest, about 3-4 hrs, behind the serum concentrations.

On the other hand, if the vegetation were 1.0 cm in diameter instead, the drug would take about 12 hours to diffuse to the center and reach the MIC, and the rise and fall of drug concentrations would be more damped, as shown in Figure 4.

Further, if the diameter of the vegetation were 2.0 cm, all this would take still longer, and the time course of the computed concentrations in the center would be as shown in Figure 5. The drug would take considerably longer, about 48 hours, to reach the MIC in the center of the vegetation, and significant growth of organisms might well take place before that. For every doubling of the diameter of the sphere, the equations show that it will take 4 times as long (the square of the ratio of the diameters) to reach an equal concentration in the center of the sphere.

### **Another Example: Simulating an Abscess or a Post-Antibiotic Effect.**

Another use for such a spherical model might, of course, be an abscess. If we could know the diffusion coefficient into abscesses of different sizes we could similarly begin to model and compute the concentrations of drug into the abscess. There might well be different diffusion coefficients through the wall, into the bulk of the abscess, and into the center. All this is theoretically capable of being determined. Effects of oxygen tension and pH upon bacterial growth and response to drugs can also be determined by careful needle aspiration done at carefully documented times just prior to incision and drainage of them, with careful cultures and determination of pH, pO<sub>2</sub>, viable organisms, and rates of growth and kill from different parts of the abscesses. In this way, useful models of events taking place within an abscess can be made, and one can see visually, in Figure 5, why abscesses much over 1 cm in diameter usually need to be incised and drained, as the diffusion into abscesses is very likely to be poorer than that seen here for endocardial vegetations.

Figure 6 shows computed drug concentrations in the center of a small sphere simulating a microorganism having a diameter of 0.1 micron, 3 simulated layers of diffusion, and a diffusion coefficient of  $1.5 \times 10^{-14}$ . This particular sphere has the property that in its center, the concentrations of drug fall below the MIC about 6 hrs after the serum levels do, thus simulating (without making any suggestions or conclusions about mechanism of action) a post-antibiotic

effect of about 6.0 hrs, as the organisms will not begin to grow again for about 6 hrs after the serum concentrations fall below the MIC.

The effects of these computed concentrations in the center of these spheres will be discussed below in the section on modeling bacterial growth and kill. We see here that the process of diffusion into and out of spherical porous objects such as endocardial vegetations and small microorganisms can be described with reasonably simple models. The equations describing this process are the same as those for release of drug from a sustained-release preparation formulation.

## MODELING BACTERIAL GROWTH AND KILL: CLINICAL APPLICATIONS

### General Considerations

Let us assume that an organism is in its logarithmic phase of growth in the absence of any antibiotic. It will have a rate constant for this growth, and a doubling time. The killing effect of the antibiotic can be modeled as a Michaelis-Menten or Hill model, which generates a rate constant for this effect. The rate of growth or kill of an organism is proportional to the difference between these two rate constants. The killing effect will be determined by the  $E_{max}$ , representing the maximum possible rate constant for kill, the  $EC_{50}$ , the concentration at which the effect is half maximal, and the time course of the serum concentrations achieved with the dosage regimen the patient is given. Both the growth rate constant and the  $E_{max}$  can be found from available data in the literature for various organisms. The general growth versus kill equation is

$$\frac{dB}{dt} = (K_g - K_k) \times B \quad (1)$$

and

$$K_k = \left( \frac{E_{max} \times C_t^n}{EC_{50}^n + C_t^n} \right) \quad (2)$$

where B is the number of organisms (set to 1 relative unit at the start of therapy), Kg is the rate constant for growth, Kk is the rate constant for killing, Emax is the maximum possible effect (rate of killing), EC50 is the concentration at which the killing rate is half maximal, n is the sigmoidicity coefficient, and Ct is the concentration at the site of the effect (serum, peripheral compartment, effect compartment, or in the center of a spherical model of diffusion), at any time t.

The EC50 can be found from the measured (or clinically estimated) minimum inhibitory concentration (MIC) of the organism. This relationship was developed by Zhi [5], and also independently by Schumitzky [6]. The MIC is modeled as a rate of kill that is equal to but opposite in direction to the rate constant for growth. The MIC thus offsets growth, and at the MIC there is neither net growth or decrease in the number of organisms. At the MIC,

$$\frac{dB}{dt} = 0, \quad \text{and } Kk = - Kg \quad (3)$$

and

$$MIC = \left( \frac{Kg \times EC50^n}{Emax - Kg} \right)^{1/n} \quad (4)$$

In this way, the EC50 can be found from the MIC, and vice versa.

The input to this effect model can be from either the central or peripheral compartment concentrations of a pharmacokinetic model, or from the center (or any other layer) of one of the spherical models of diffusion. The sphere may represent an endocardial vegetation, an abscess, or even a small microorganism. In the latter case, one can adjust the sphere diameter and the diffusion coefficient so that the concentrations in the center of the small sphere lag behind the serum concentrations and cross below the MIC about 6 hours after the serum concentrations do, to simulate a post-antibiotic effect of about 6 hours, for example. The effect relationship was modeled by Bouvier D'Ivoire and Maire [7], from data obtained from Craig [8], for pseudomonas and an aminoglycoside.

Let us first examine these effect models with relationship to the dosage regimen of amikacin developed in the previous paper on analyzing concentrations in spherical diffusion models. In that paper we had considered a hypothetical 65 year old man, 70 in tall, weighing 70 kg, having a serum creatinine of 1.0 mg/dL. We also assumed that he had a vegetation on his aortic valve, seen by echocardiography, that might be either 0.5, 1.0, or 2.0 cm in diameter, and we wanted to examine the ability of an amikacin regimen designed to achieve serum peaks of 45 and troughs of about 5 ug/ml to reach effective concentrations within the vegetation in these three cases. We applied the findings of Bayer et al [9,10] to predict the time course of amikacin concentrations in the center of the above three different vegetations. Let us now examine the results of these analyses.

The patient's dosage regimen consisted of an initial dose of 850 mg of amikacin followed by 750 mg every 12 hours thereafter. On that regimen, predicted serum concentrations were 43 ug/ml for the peak and 3.2 for the trough, possibly a bit low, as the MIC of the organism was stated to be 8.0 ug/ml. The computed concentration of amikacin in the various vegetations was shown in the previous paper. Figure 7 is a plot not only of the predicted time course (the first six days) of serum amikacin concentrations for the patient described here, but also of its ability to kill microorganisms using the model made by Maire, based on the data of Craig. In Figure 7 there is no assumption of any post-antibiotic effect. The serum concentration profile alone is presented as the input to the bactericidal effect model.

The model always assumes an initial inoculum of one relative unit of organisms. The scale of the relative number of organisms is shown on the right side of Figure 7, while the scale of the serum concentrations is on the left. As shown in the figure, the serum concentration profile resulting from that regimen appears to be able to kill such an organism well in this particular patient. As the serum concentrations fall below the MIC with the first dose, however, the organisms begin to grow again, but the second dose kills them again, with slight regrowth once again toward the end of that dose interval. The third dose reduces the number of organisms essentially to zero. Use of this effect model suggests that such a serum concentration profile should be effective in killing an organism having an MIC of 8.0 ug/ml, even though the serum

concentrations are below the MIC about one third of the time, as the high peaks are effective in the killing.

Figure 8 now shows the computed results in the center of the simulated endocardial vegetation having a diameter of 0.5 cm. The solid line shows the computed time course of amikacin which has diffused into the center of the vegetation. The dotted line again represents the computed relative number of organisms. Here the organisms grow almost 4-fold, to almost four relative units, before the concentrations in the center of the vegetation reach the MIC, after which killing begins. The organisms are reduced essentially to zero by 24 hours, suggesting that such a regimen would probably kill well in the center of an endocardial vegetation of approximately 0.5 cm diameter.

Figure 9 is a similar plot, but for the simulated vegetation having a diameter of 1.0 cm. Things here are not quite so good. There is a significant lag time of about 3 to 4 hours before visible concentrations are reached in the center of the vegetation. The MIC is not reached until approximately 10 hours. During that time, the number of organisms has increased from one to approximately 150 relative units. However, after the MIC is reached, killing begins, although not quite so rapidly as with the smaller vegetation, due to the slower rate of rise of drug concentration in the center of the larger vegetation. However, killing appears to be essentially complete after approximately 40 hours. This suggests that the above regimen may be adequate to kill in the center of a 1.0 cm vegetation, but perhaps does so with less confidence of success than with the vegetation of 0.5 cm diameter. The doubt about this is suggested by the slower rate of killing and by the longer time required to reduce the number of organisms essentially to zero.

As shown in Figure 10, things are much worse for the simulated endocardial vegetation of 2.0 cm. Diffusion into the center is a great deal slower. Visible concentrations are not achieved until after approximately 12 hours have elapsed, and about 48 hours are required before they reach the MIC. During this time, the number of organisms has increased astronomically, from 1 relative unit to over 1 million such units. However, after about five days, due to the continued presence of concentrations in the center of the vegetation approaching 12 to 15 ug/ml, killing in fact does seem to take place, and after about six days the number of organisms appears to be



close to zero. However the behavior of this model strongly suggests that such a dosage regimen might very likely be inadequate in the center of a 2.0 cm simulated vegetation and might, at a minimum, require much more aggressive therapy with higher doses and serum concentrations, surgery, much more prolonged therapy, or all of these.

Figure 11 shows the computed concentrations in the small hypothetical microorganism used in the previous paper to simulate the time course of the post-antibiotic effect (PAE). There is a lag of about 6 hours between the fall of the serum concentrations and that of the concentrations in the center of this hypothetical microorganism. Because of this, if the dosage interval were to be greater so that the concentrations in the hypothetical microorganism would fall below the MIC, one would see that they would do so approximately six hours after the serum concentrations fall below the MIC, thus simulating a post-antibiotic effect of approximately six hours.

What would be the contribution (if any) of such a PAE to overall therapy? As shown in Figure 12, the outcome is not very different from that shown in Figure 7. In both cases, killing is rapid and prompt. One can see that due to the diffusion model, there may be a delay of approximately six hours before the concentrations in the hypothetical microorganism reach the MIC. During that time, the number of organisms has grown from 1 to about 5.4 relative units. However, after that time, the concentrations are always above the MIC, and killing at a significant rate begins and continues, with the organisms being reduced essentially to zero by about 36 hours.

### **An Interesting Case**

These diffusion and effect models were of interest when they were used to analyze data obtained much earlier, back in 1991, from a patient in Christchurch, New Zealand, seen through the courtesy of Dr. Evan Begg. The patient had a pyelonephritis and received tobramycin, 80 mg approximately every 8-12 hours. He was having a satisfactory clinical response to therapy when, on about the 6th day of therapy, he suddenly and unexpectedly relapsed and went into septic shock. He then received much more aggressive tobramycin, and eventually recovered. The MIC of his organism was 2.0 ug/ml. The analysis described below was not done until several years

later, after the models of diffusion and growth and kill had been developed. At that later time, this interesting patient's data was analyzed retrospectively.

Figure 13 shows the computed concentrations of drug in the center of the 0.1 micron sphere representing an organism having the PAE of 6 hours, in the patient's first phase, when he appeared to be a general medical patient (not an ICU patient) having a satisfactory clinical response to his tobramycin therapy. However, at the end of this time (from 120-148 hours into therapy) he unexpectedly relapsed on about day 6 of therapy, went into septic shock, and clearly became an ICU patient.

Note the damped response in the center of the small sphere to the sharp peaks and troughs of the serum concentrations. While one may have many different views as to what the mechanism of the PAE is, this diffusion model appears to do a reasonable job of describing the effect itself. As data accumulate about diffusion into endocardial vegetations and abscesses, this diffusion model will permit modeling of these events during a patient's clinical care in a way that is now becoming possible.

Now, consider the computed rate of growth and kill of his organisms during his treatment. We have a hint in that his peak serum concentrations were low, only about 5.0 ug/ml. His measured serum peak was 4.5 ug/ml, and his trough was 0.4 ug/ml. Figure 14 describes the growth and kill of the organisms in response to events in his serum concentration compartment, while Figure 15 shows the same events as viewed with the sphere model simulating the PAE.

Note in both figures that there appear to be few organisms present at the outset of therapy. Growth becomes significant and visible in Figure 14 after the first hiatus between doses, and then becomes exponential during day 6 of therapy, after the last dose on that plot, which ends just before the next dose which was given during his next period, that of septic shock.

Figure 15 extends this examination to the possible contribution of the PAE, where the concentrations in the center of the small sphere shown above using the sphere model are now evaluated with respect to their ability to kill the organisms. Note again that the regimen appeared

to be effective at first, but that the organisms grew out again exponentially when the concentrations fell significantly below the MIC for a significant time. The exponential growth of organisms escaping from control as shown in Figures 14 and 15 correlated well with the patient's clinical relapse at just that time, with development of septic shock.

Figure 16 shows the subsequent course of this patient when he was in his next phase of acute urosepsis. There was essentially no carry-over of drug from the last dose shown in Figures 13 to 15 to the patient's next dose, which was given at time zero in Figure 16. That figure shows the many serum concentrations measured during this phase of his hospital course. It also shows the results of Bayesian fitting of the population model of tobramycin as it is in ICU patients, with its much larger central volume of distribution (now that he had become a seriously ill ICU patient) in both his central (serum) and peripheral (nonserum) compartments. During this time, the patient's serum creatinine also rose from 0.7 to 3.7 mg/dL.

One can see that it took about two days, as new serum concentrations were obtained, for ward personnel to react to his suddenly much increased volume of distribution (from 0.18 to 0.51 L/kg as he changed from being a general medical patient to being a seriously ill ICU patient) and to his much decreased renal function, and to give him the much greater doses required to achieve effective peak serum concentrations of about 8 to 9 ug/ml. Note also that his trough concentrations rose from about 0.3 up to 2.0 ug/ml during this time, so that the time that serum concentrations were below the MIC was greatly reduced.

Figure 17 shows the computed concentrations in the center of the small sphere simulating the PAE. As shown, the concentrations barely reach the MIC on the 3rd day (48-72 hours), but are at least the MIC from about 84 hours onward.

Figure 18 shows the plot of the computed bacterial growth and kill based on the input from the serum concentration profile during this time, without any aid from the simulated PAE. The organisms grow out of control in the first two days (again correlating with the patient's relapse into sepsis the day before, and the time required for ward personnel to perceive the problem and to adjust his dosage sharply upward to achieve serum peaks in the range of 7 to 9

ug/ml). As these higher and more effective concentrations were maintained, however, bacterial killing could finally be seen at about the sixth day in this figure, and appeared to be effective after that, correlating with the patient's subsequent clinical recovery.

Figure 19 shows the same events, but now using the diffusion model of the small microorganism and its simulated PAE. Using this model, killing can be seen to begin slightly earlier, at about the fifth day in the figure, and also to be effective after that.

In general, models of bacterial growth and kill permit one to incorporate known in vitro data of the logarithmic growth rate of the organism and the maximum kill rate achieved with the antibiotic, to integrate it with data of the MIC of each individual patient's organism, and to model the growth and decline of the relative numbers of organisms. These Zhi models have correlated well, in this patient, with his unexpected relapse from having an apparently satisfactory response to therapy to becoming a seriously ill patient with septic shock, and with his subsequent recovery later on, as effective serum concentrations were achieved and maintained.

The Zhi model does not describe the decline of growth seen over time, reaching a maximum number of organisms, as found by Mouton, Vinks, and Punt [9]. The organisms are always assumed to be in their logarithmic growth phase, the maximum possible. In addition, the model does not account for the increase in bacterial resistance found with time, and the emergence of resistant organisms. However, one can use the maximum possible MIC which the organism is expected to reach, and examine the behavior of the model. In this case, the Zhi model becomes a useful example of the "worst case" scenario, with the resistant organisms being so from the very beginning of therapy, and with the logarithmic growth rate always being in effect, never slackening. If a given dosage regimen, generating a certain serum concentration profile, can kill well using the Zhi model, one might expect it to be likely to do at least as well in clinical circumstances, where the growth rate may (or may not) slacken with time and may (but may not) reach a maximum number of organisms, and the resistant organisms emerge more slowly with time.

Clearly, further work in this area is needed, but models of this type are beginning to provide a useful new way to perceive, analyze, and evaluate the efficacy of antibiotic therapy. Similar approaches may also be useful in analyzing therapy of patients with AIDS, using the PCR assays, and with cancer.

#### ACKNOWLEDGMENTS

Supported by US Government grants LM 05401, RR 11526, and RR 01629, and by the Stella Slutzky Kunin Research Fund.

#### References.

1. Maire P, Barbaut X, Vergnaud JM, El Brouzi M, Confesson M, Pivot C, Chuzeville M, Ivanoff N, Brazier J, and Jelliffe R: Computation of Drug Concentrations in Endocardial Vegetations in Patients during Antibiotic Therapy. *Int. J. Bio-Med. Comput.*, 36: 77-85, 1994.
2. Bayer A, Crowell D, Yih J, Bradley D, and Norman D: Comparative Pharmacokinetics and Pharmacodynamics of Amikacin and Ceftazidime in Tricuspid and Aortic Vegetations in Experimental *Pseudomonas* Endocarditis. *J. Infect. Dis.*, 158: 355-359, 1988.
3. Bayer A, Crowell D, Nast C, Norman D, and Borelli R: Intravegetation Antimicrobial Distribution in Aortic Endocarditis Analyzed by Computer-Generated Model: Implications for Treatment. *Chest*, 97: 611-617, 1990.
4. Jelliffe R, Schumitzky A, Van Guilder M, and Jiang F: User Manual for version 10.7 of the USC\*PACK Collection of PC Programs, USC Laboratory of Applied Pharmacokinetics, December 1, 1995.

5. Zhi J, Nightingale CH, and Quintiliani R: Microbial Pharmacodynamics of Piperacillin in Neutropenic Mice of Systemic Infection due to *Pseudomonas Aeruginosa*. *J Pharmacokin. Biopharm.* 4: 355-375, 1988.
6. Schumitzky A: personal communication.
7. Bouvier D'Ivoire M, and Maire P: Dosage Regimens of Antibacterials: Implications of a Pharmacokinetic/Pharmacodynamic Model. *Drug Invest.* 11: 229-239, 1996.
8. Craig W, and Ebert S: Killing and Regrowth of Bacteria in Vitro: a Review. *Scand J Infect Dis Suppl* 74: 63-70, 1991.
10. Mouton J, Vinks AATMM, and Punt N: Pharmacokinetic-Pharmacodynamic Modeling of Ceftazidime during Continuous and Intermittent Infusion. Chapter 6, pp 95-110, in the Ph.D. Thesis of Vinks AATMM: Strategies for Pharmacokinetic Optimization of Continuous Infusion Therapy of Ceftazidime and Aztreonam in Patients with Cystic Fibrosis, November, 1996.

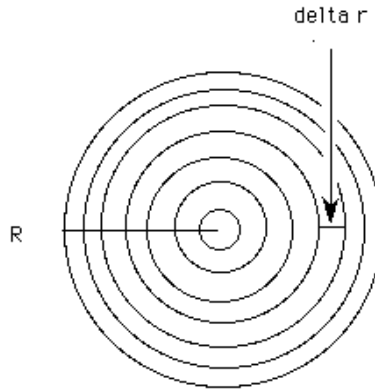


Figure 1. Diagram of the concentric layers of the spherical model of the endocardial vegetation.

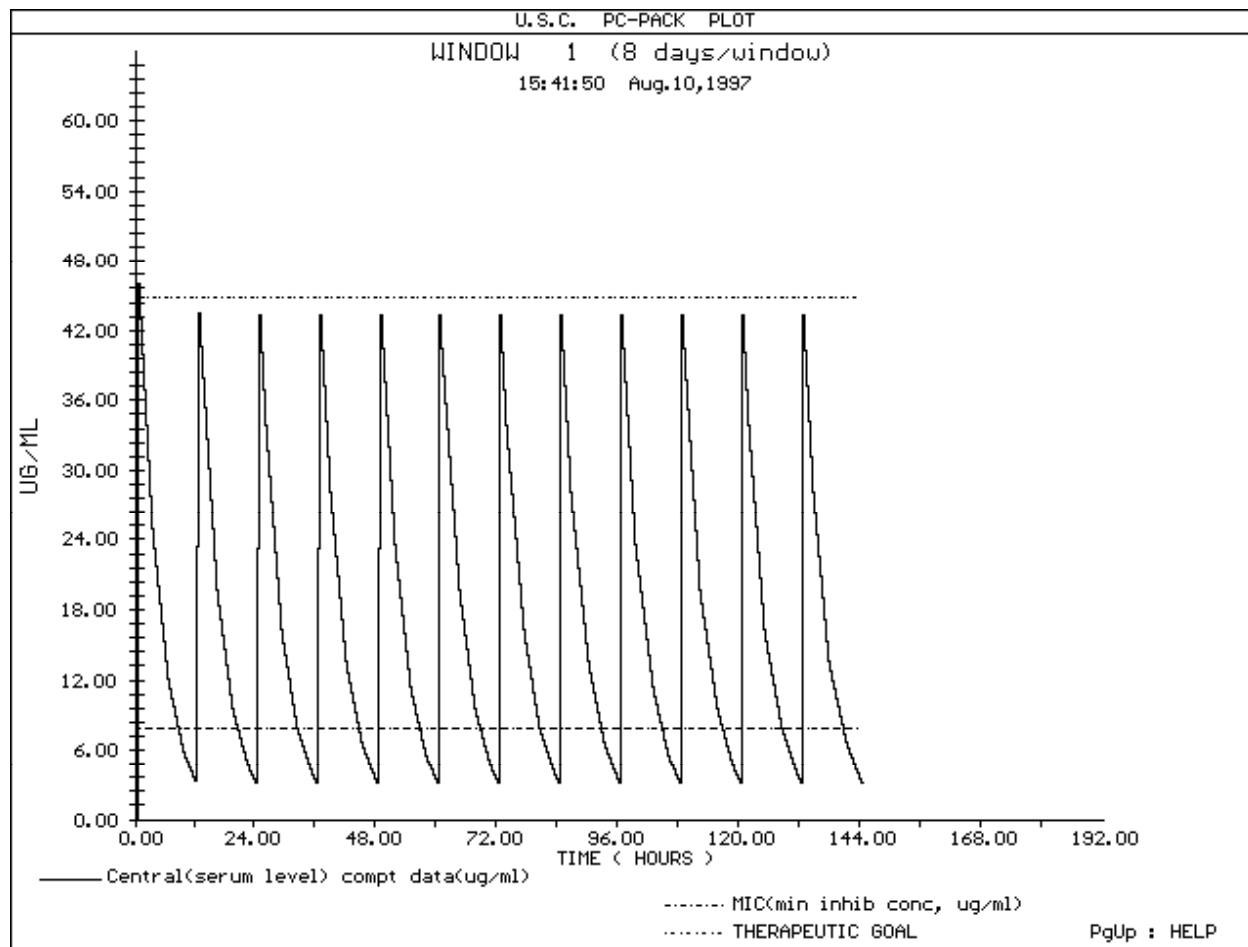


Figure 2. Predicted time course (the first 6 days) of serum Amikacin concentrations for the patient described. Upper horizontal dotted line - initial stated target peak serum concentration of 45 ug/ml. Lower horizontal dashed line - the estimated organism MIC of 8.0 ug/ml.



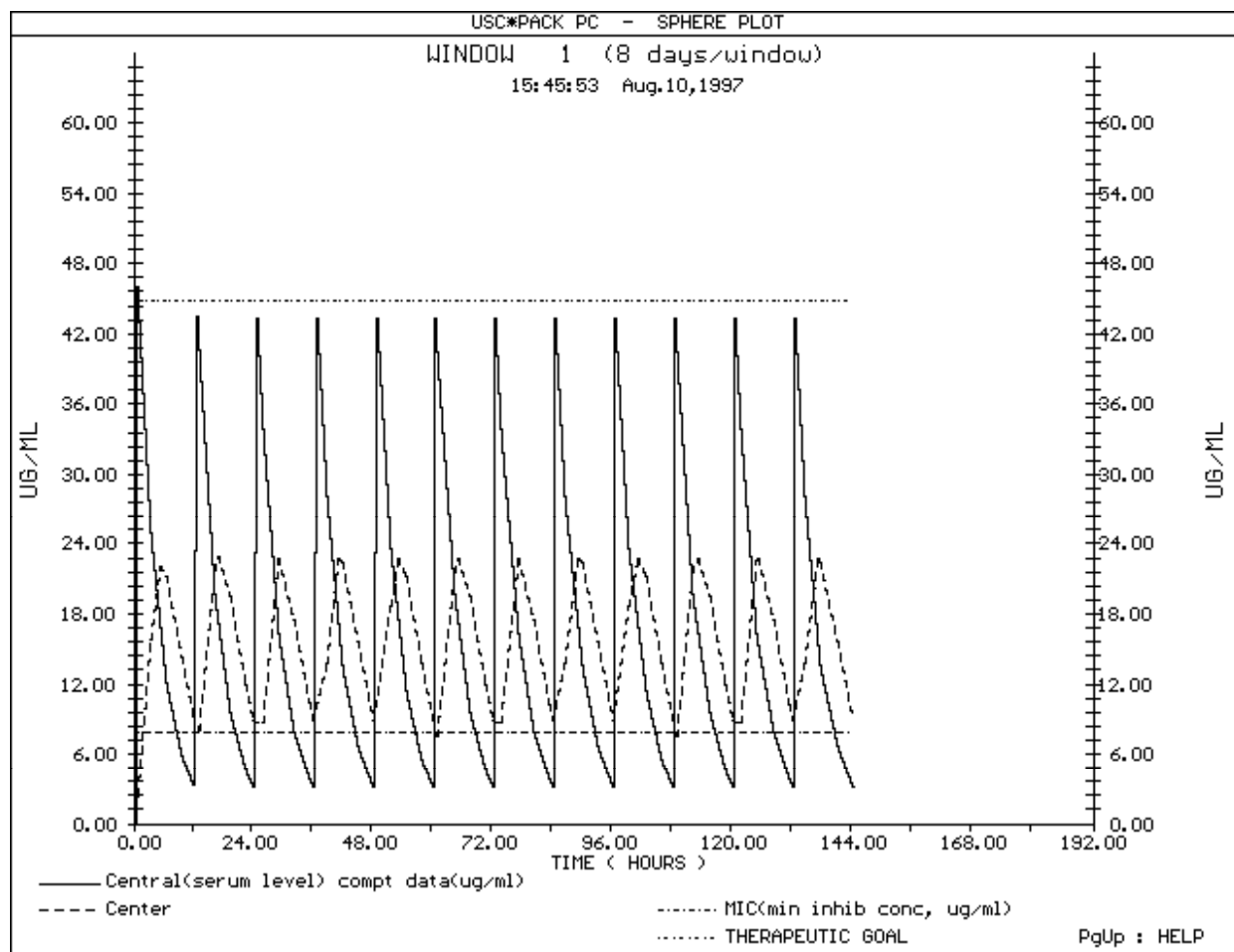


Figure 3. Predicted time course (the first 6 days) of Amikacin concentrations (dashed line) in the center of a simulated endocardial vegetation of 0.5 cm. Solid line - Predicted serum concentrations, and other lines and symbols as in Figure 2. The predicted endocardial concentrations rise promptly, and are consistently above the estimated MIC of 8.0 ug/ml.

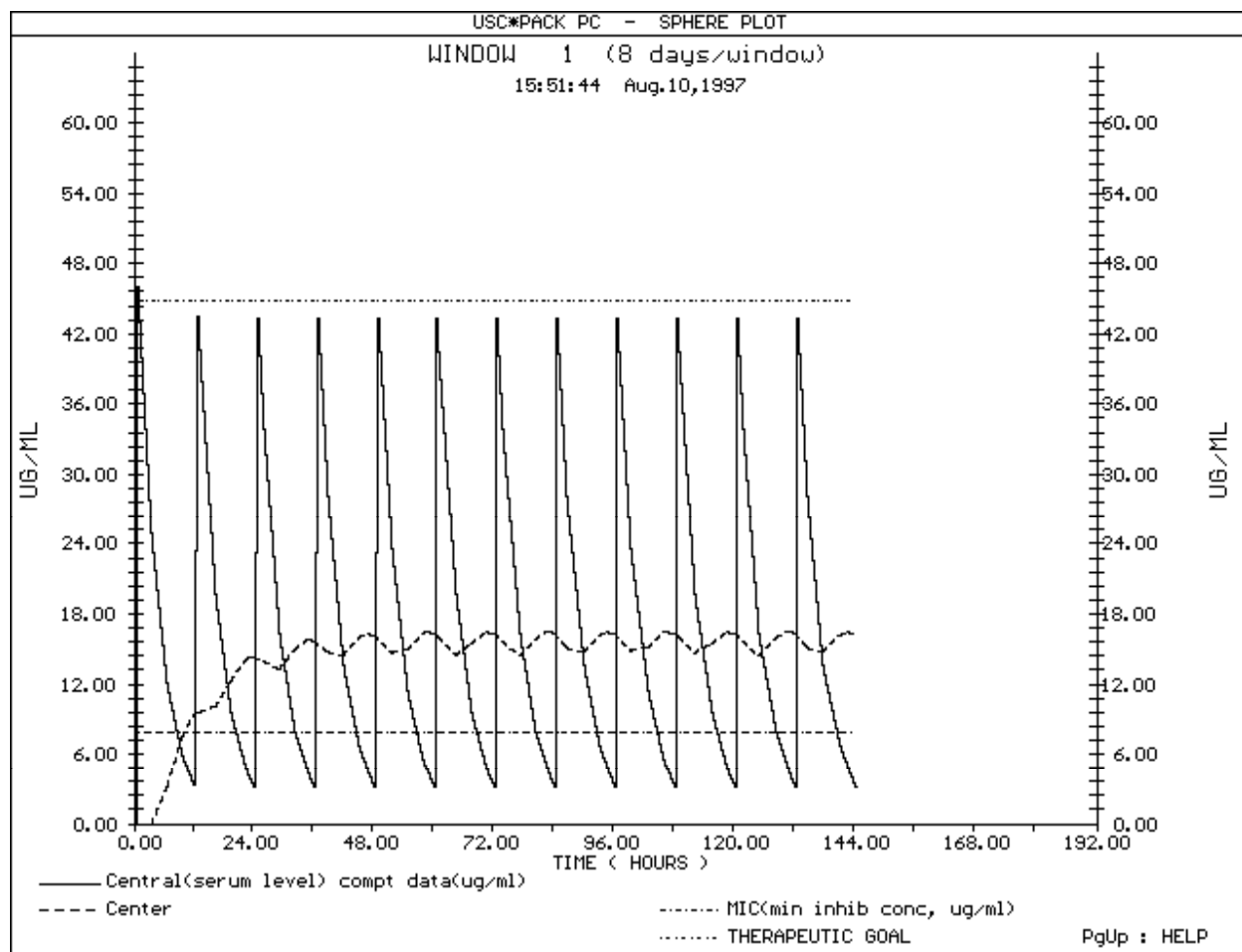


Figure 4. Predicted time course (the first 6 days) of Amikacin concentrations (dashed line) in the center of a simulated endocardial vegetation of 1.0 cm. Solid line - Predicted serum concentrations, and other lines and symbols as in Figure 2. The predicted endocardial concentrations rise more slowly, are more damped, with smaller oscillations from peak to trough, but once the estimated MIC is reached, are consistently above 8.0 ug/ml.

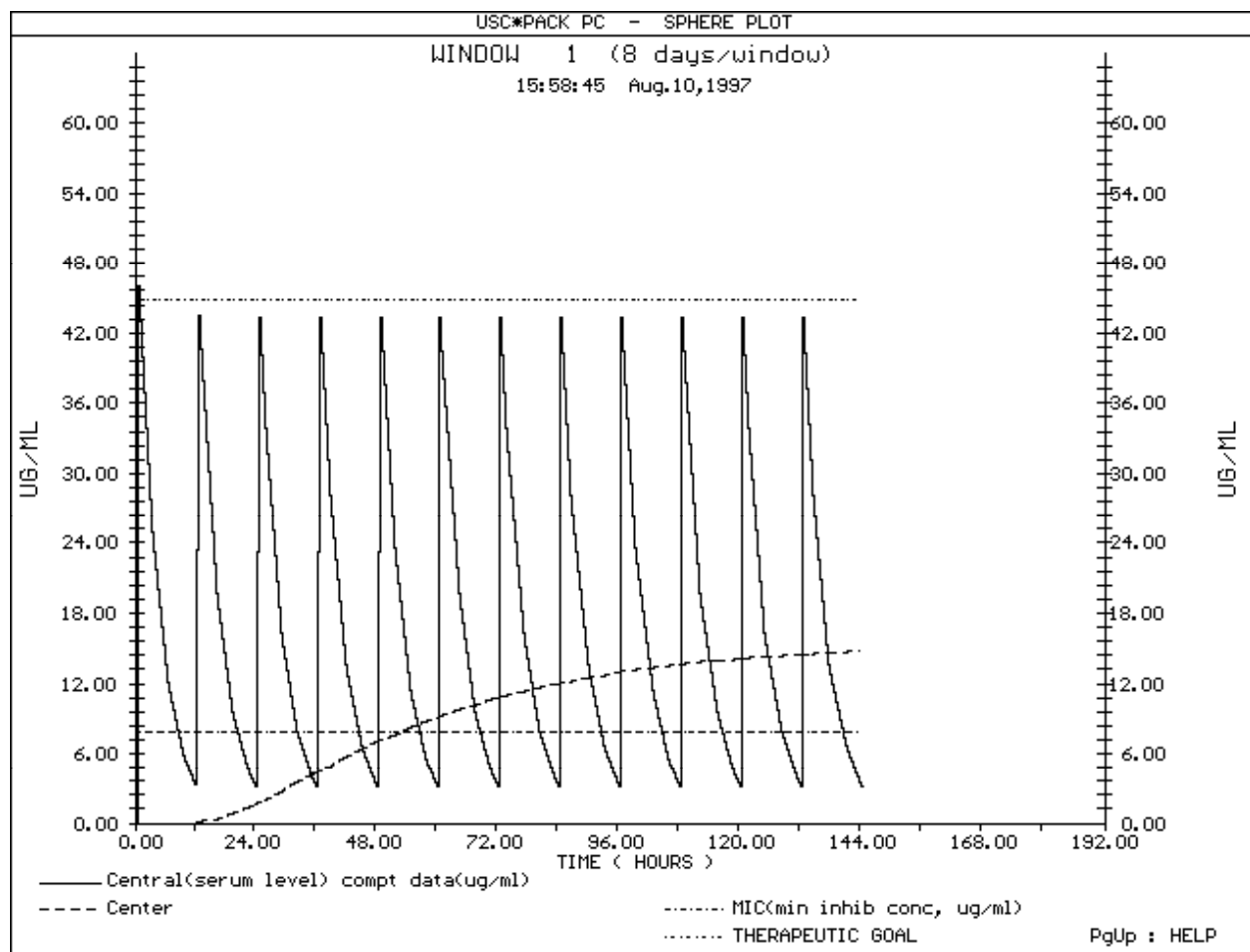


Figure 5. Predicted time course (the first 6 days) of Amikacin concentrations (dashed line) in the center of a simulated endocardial vegetation of 2.0 cm. Solid line - Predicted serum concentrations, and other lines and symbols as in Figure 2. The predicted endocardial concentrations rise much more slowly and are much more damped, with essentially no oscillations from peak to trough. Once the estimated MIC is reached, the concentrations are consistently above 8.0 ug/ml, but two full days are required before the MIC is reached.

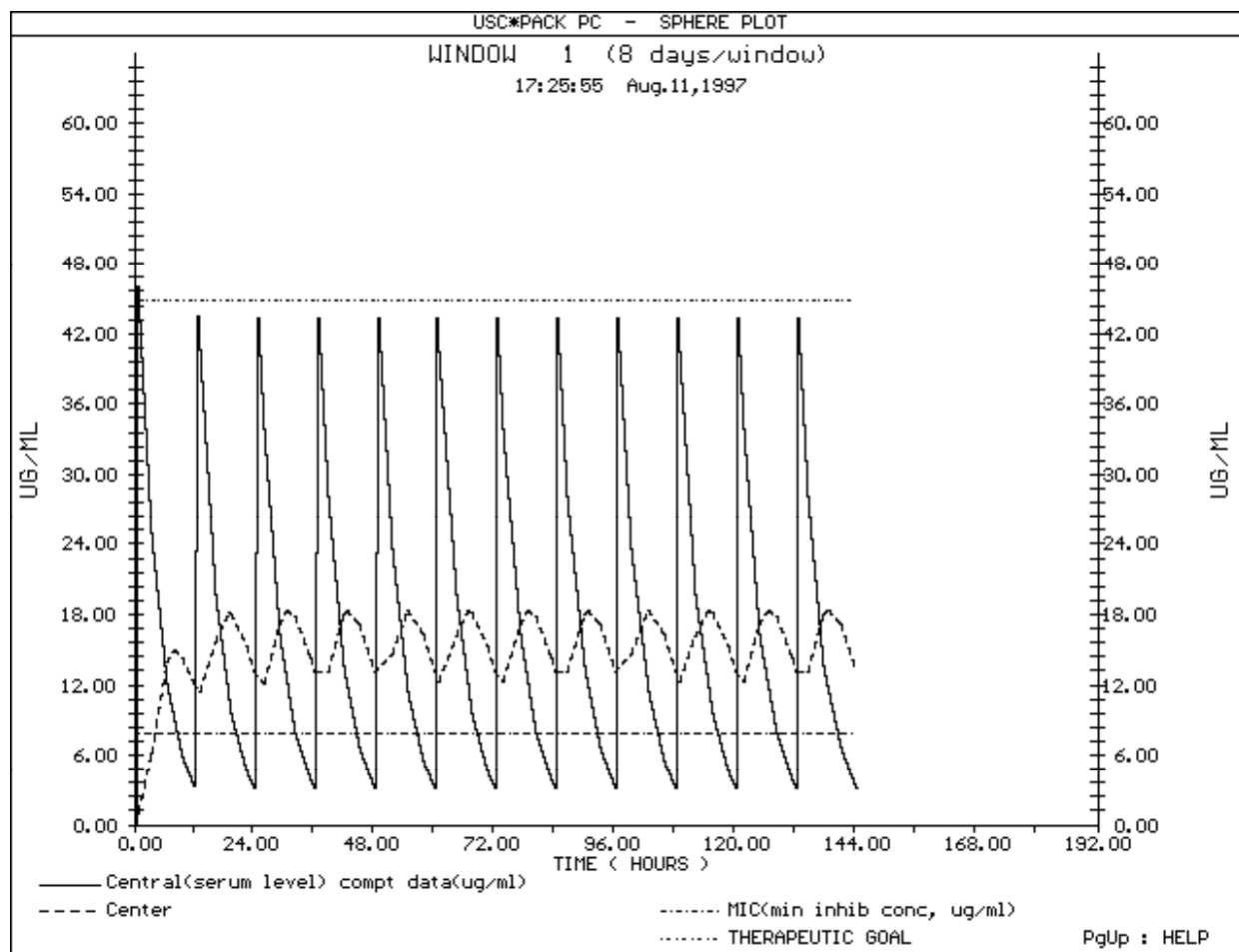


Figure 6. Plot of computed amikacin concentrations (the first 6 days) in the center of a simulated microorganism. Parameters in the sphere diffusion model are adjusted so that concentrations in the center of the organism lag behind the serum concentrations and, if they fall below the MIC, would do so approximately 6 hrs after the serum concentrations do, thus simulating a post-antibiotic effect of about 6 hrs.

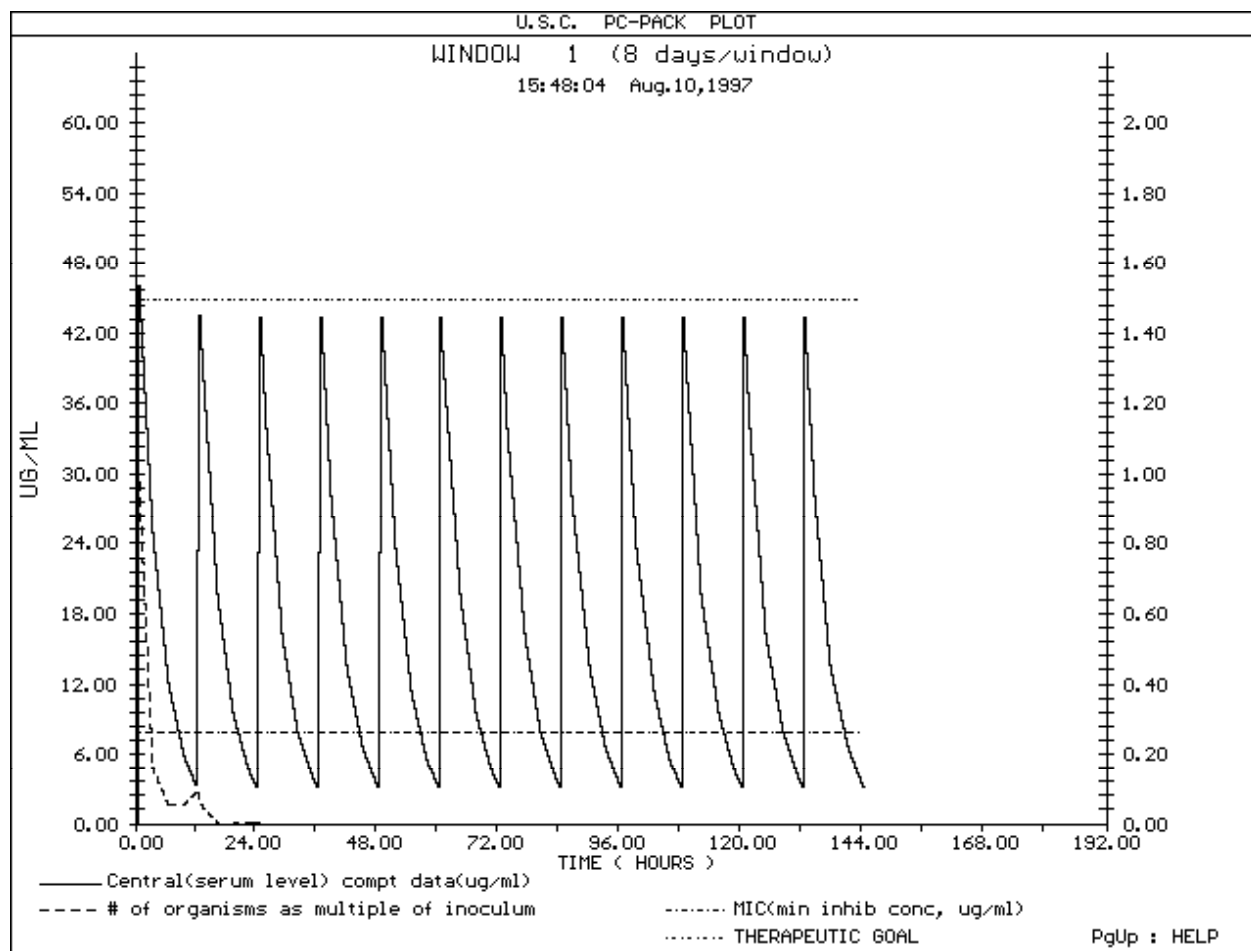


Figure 7. Predicted Killing effect of the regimen. Input from the central (serum) compartment profile of serum concentrations. The regimen is likely to kill well for a bloodstream infection (sepsis). Solid line and left hand scale - serum concentrations. Dashed line and right hand scale - relative numbers of organisms, with 1.0 relative unit present at the start of therapy. Upper horizontal dotted and dashed line - original peak serum goal of therapy. Lower horizontal dashed line: the patient's MIC of 2.0 ug/ml.

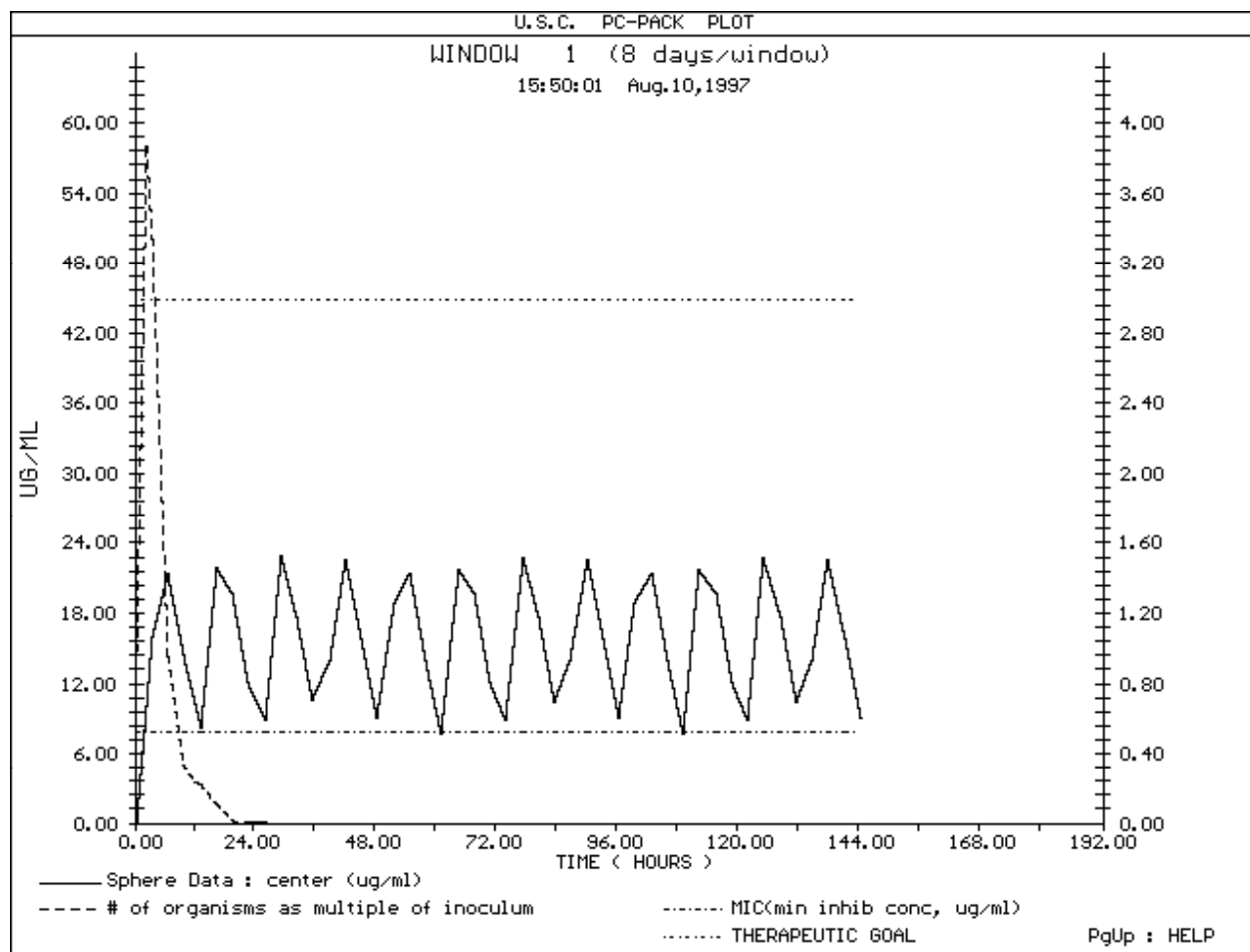


Figure 8. Killing effect as predicted in the center of the 0.5 cm diameter vegetation. Good and fairly prompt killing is seen. Solid line and left hand scale - drug concentrations in the center of the vegetation. Dashed line and right hand scale - relative numbers of organisms, with 1.0 relative unit present at the start of therapy. Upper horizontal dotted and dashed line - original peak serum goal of therapy. Lower horizontal dashed line: the patient's MIC of 2.0 ug/ml.

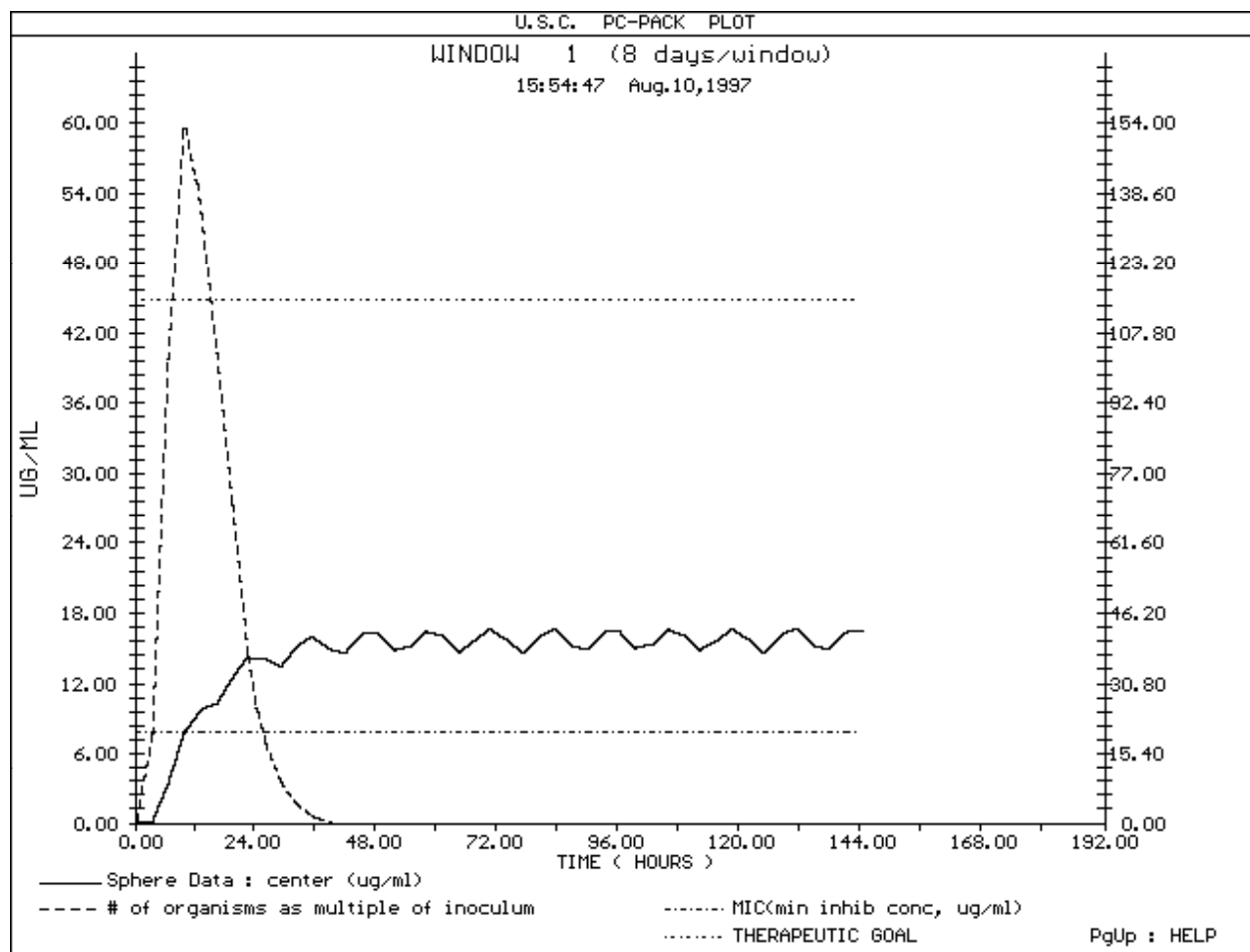


Figure 9. Killing effect computed for the center of a simulated vegetation with 1.0 cm diameter. The effect is delayed due to the slower diffusion into the center, but finally became adequate. Solid line and left hand scale - drug concentrations in the center of the vegetation. Dashed line and right hand scale - relative numbers of organisms, with 1.0 relative unit present at the start of therapy. Upper horizontal dotted and dashed line - original peak serum goal of therapy. Lower horizontal dashed line: the patient's MIC of 2.0 ug/ml.

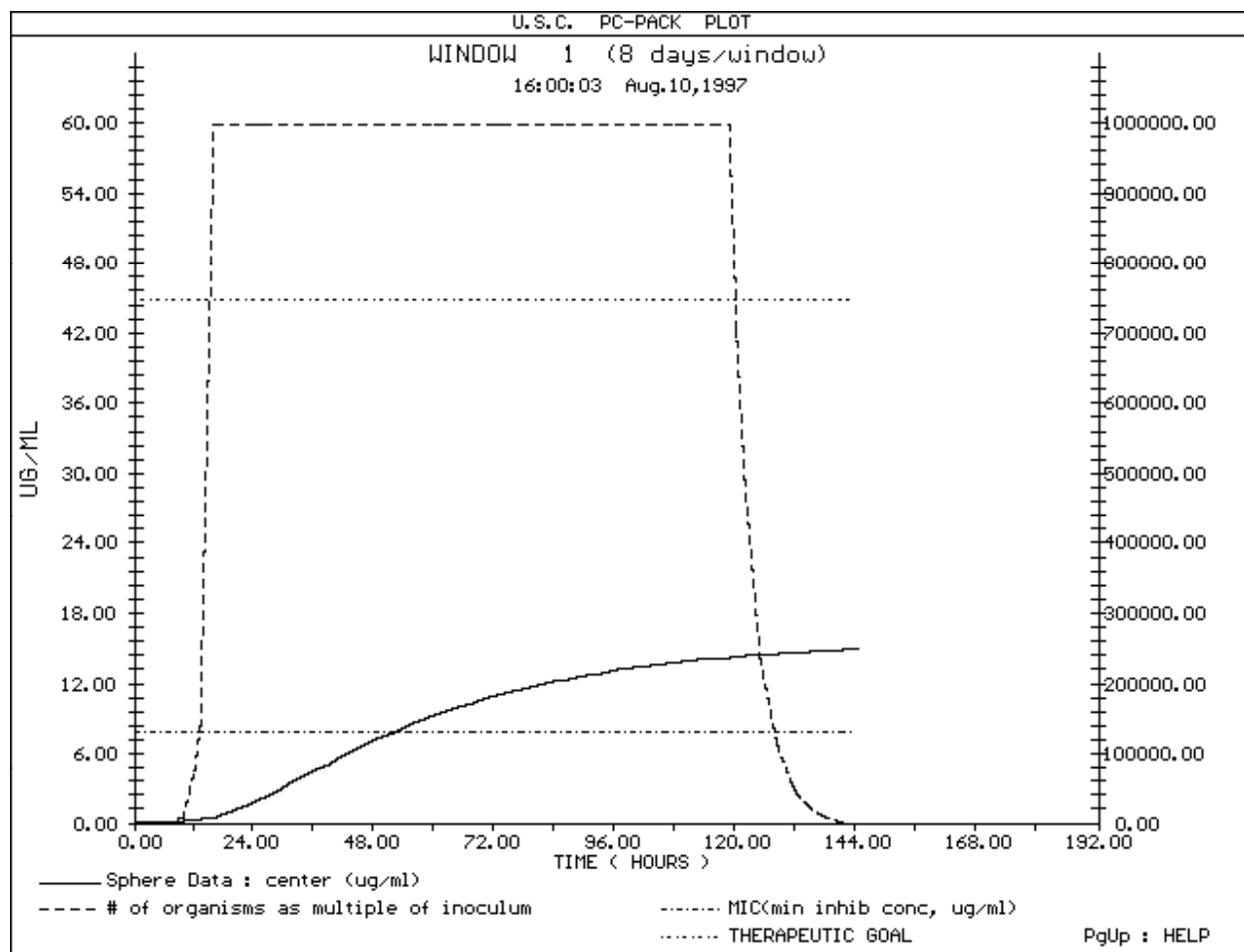


Figure 10. Killing effect computed for the center of a 2.0 cm simulated vegetation. Diffusion to the center is much prolonged while bacterial growth continues. Killing is delayed very significantly. Solid line and left hand scale - drug concentrations in the center of the vegetation. Dashed line and right hand scale - relative numbers of organisms, with 1.0 relative unit present at the start of therapy. Upper horizontal dotted and dashed line - original peak serum goal of therapy. Lower horizontal dashed line: the patient's MIC of 2.0 ug/ml.



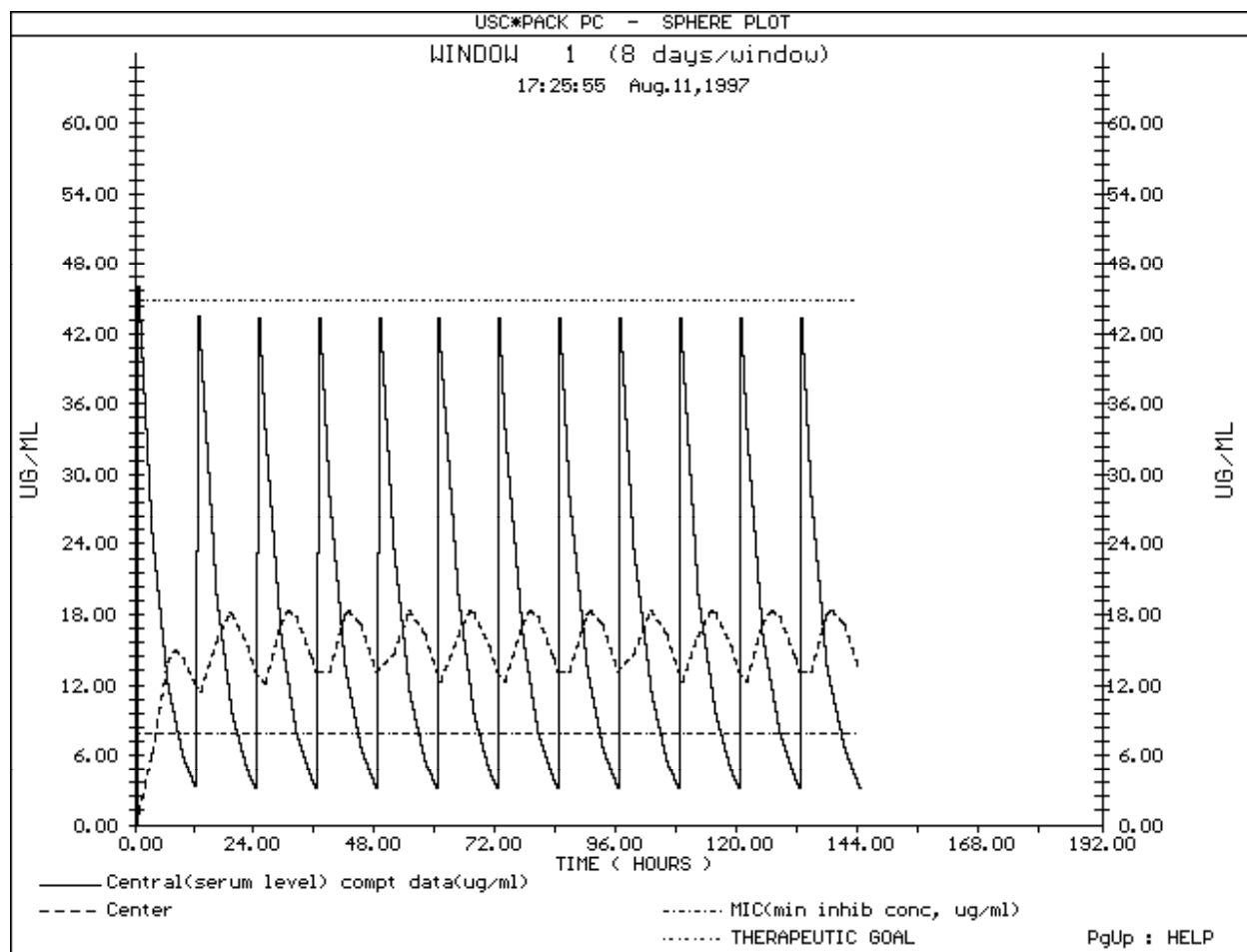


Figure 11. Computed amikacin concentrations in the center of a hypothetical microorganism in which concentrations fall below the MIC about 6 hr after the serum concentrations do, thus simulating (regardless of mechanism) a post-antibiotic effect of about 6 hrs. Solid line and left hand scale - serum drug concentrations. Dashed line and right hand scale - computed concentrations in the center of the microorganism simulating the post-antibiotic effect. Upper horizontal dotted and dashed line - original peak serum goal of therapy. Lower horizontal dashed line: the patient's MIC of 2.0 ug/ml.

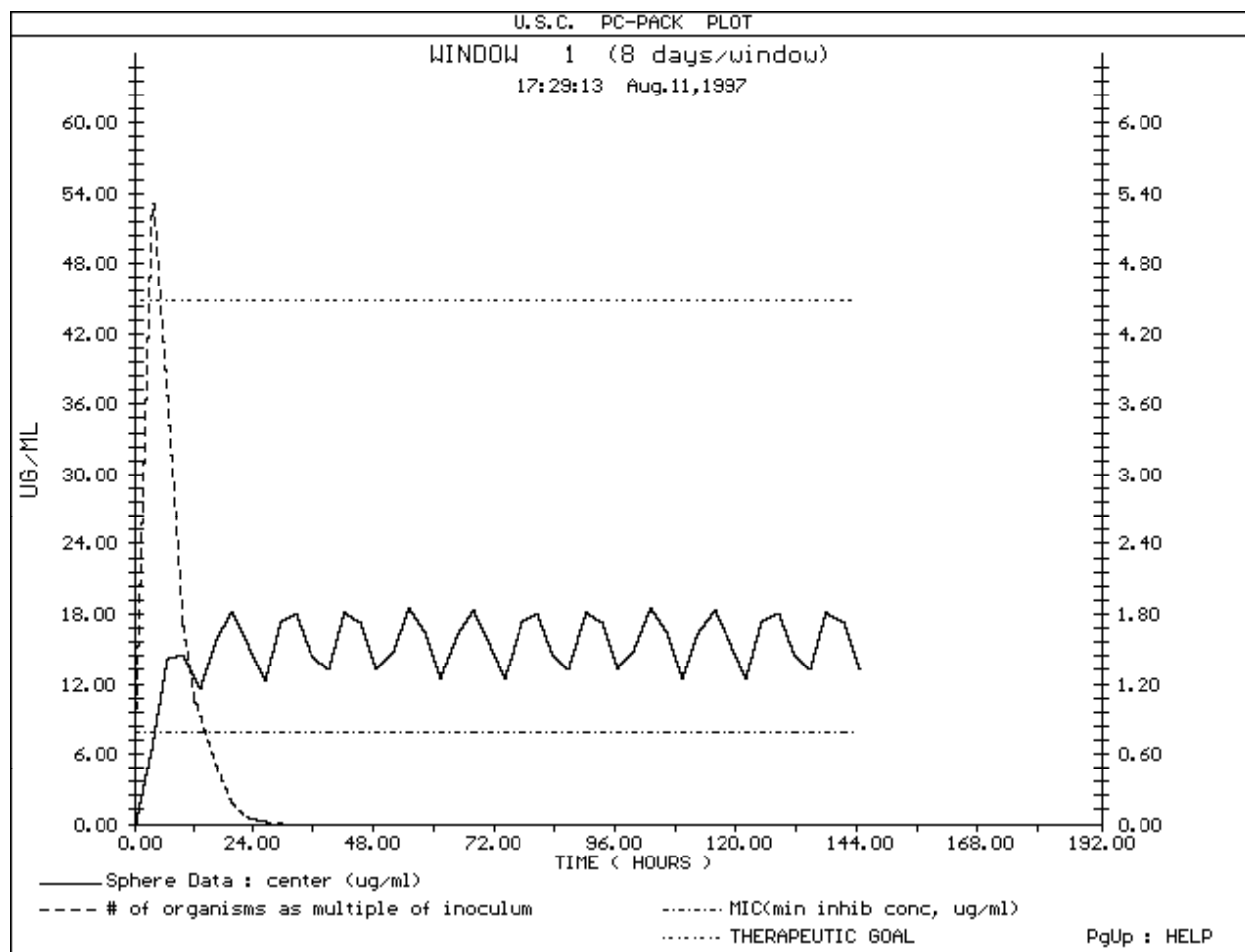


Figure 12. Killing effect predicted for the simulated post-antibiotic effect of 6 hrs, using the computed concentrations in the center of the simulated microorganism as input to the effect model. Solid line and left hand scale - drug concentrations in the center of the microorganism simulating the post-antibiotic effect. Dashed line and right hand scale - relative numbers of organisms, with 1.0 relative unit present at the start of therapy. Upper horizontal dotted and dashed line - original peak serum goal of therapy. Lower horizontal dashed line: the patient's MIC of 2.0 ug/ml.

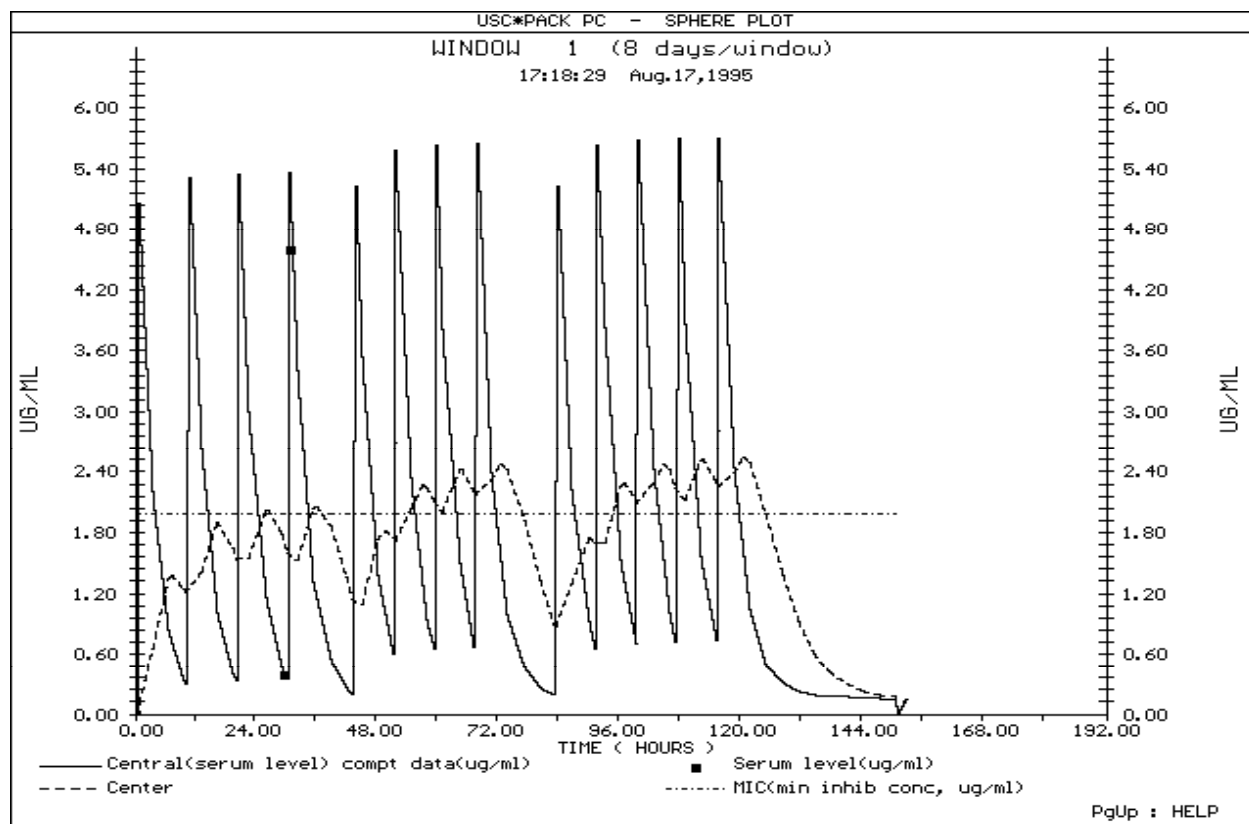


Figure 13. Patient receiving Tobramycin. This figure shows the measured serum concentrations (small rectangles), and the Bayesian fitted model. Small solid rectangles - measured serum concentrations. Solid line and left hand scale - fitted serum drug concentrations. Dashed line and right hand scale - concentrations in the small organism simulating the post-antibiotic effect. Horizontal dashed line: the patient's MIC of 2.0 ug/ml.

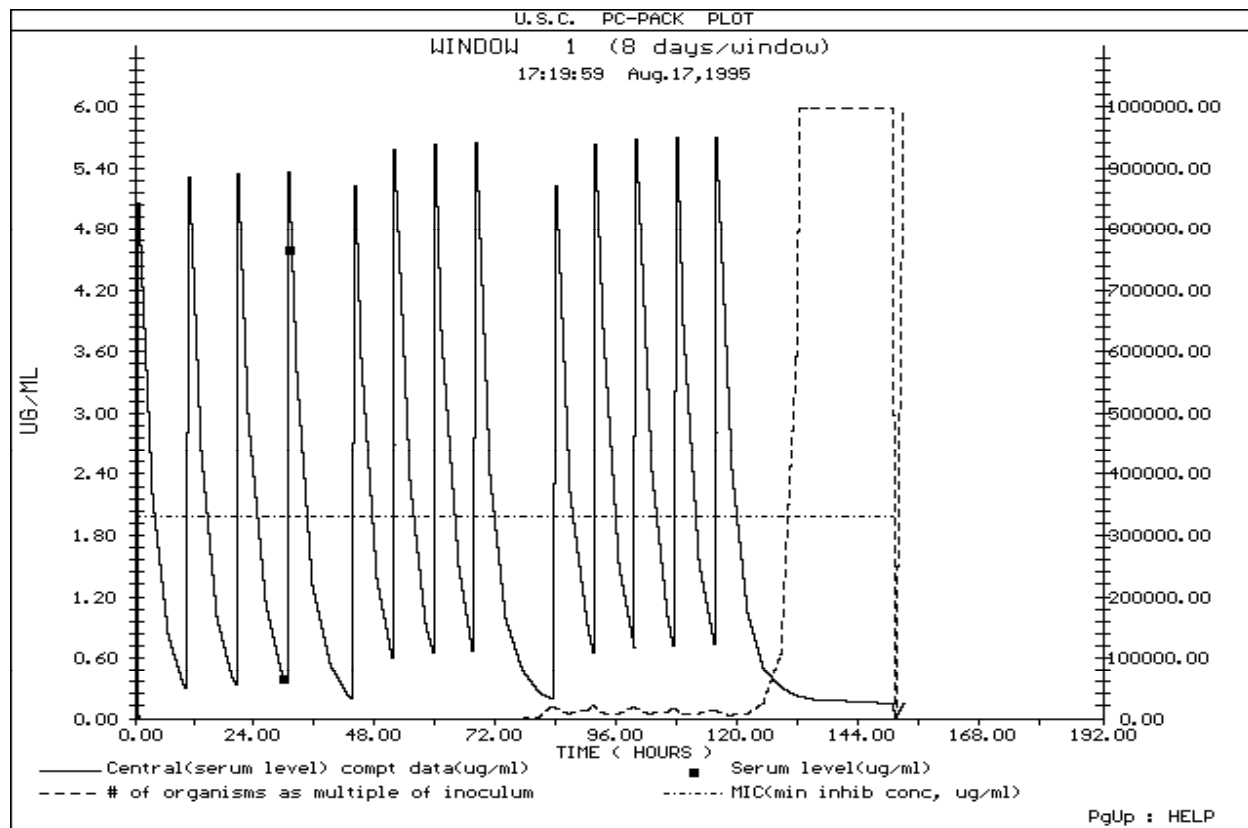


Figure 14. Patient receiving Tobramycin. This figure shows the measured serum concentrations (small solid rectangles), and his individualized Bayesian fitted model. Solid line and left hand scale: fitted serum drug concentrations. Dashed line and right hand scale: relative numbers of organisms. The plot always begins with 1.0 relative units of organism. Horizontal dashed line: the patient's MIC of 2.0 ug/ml.

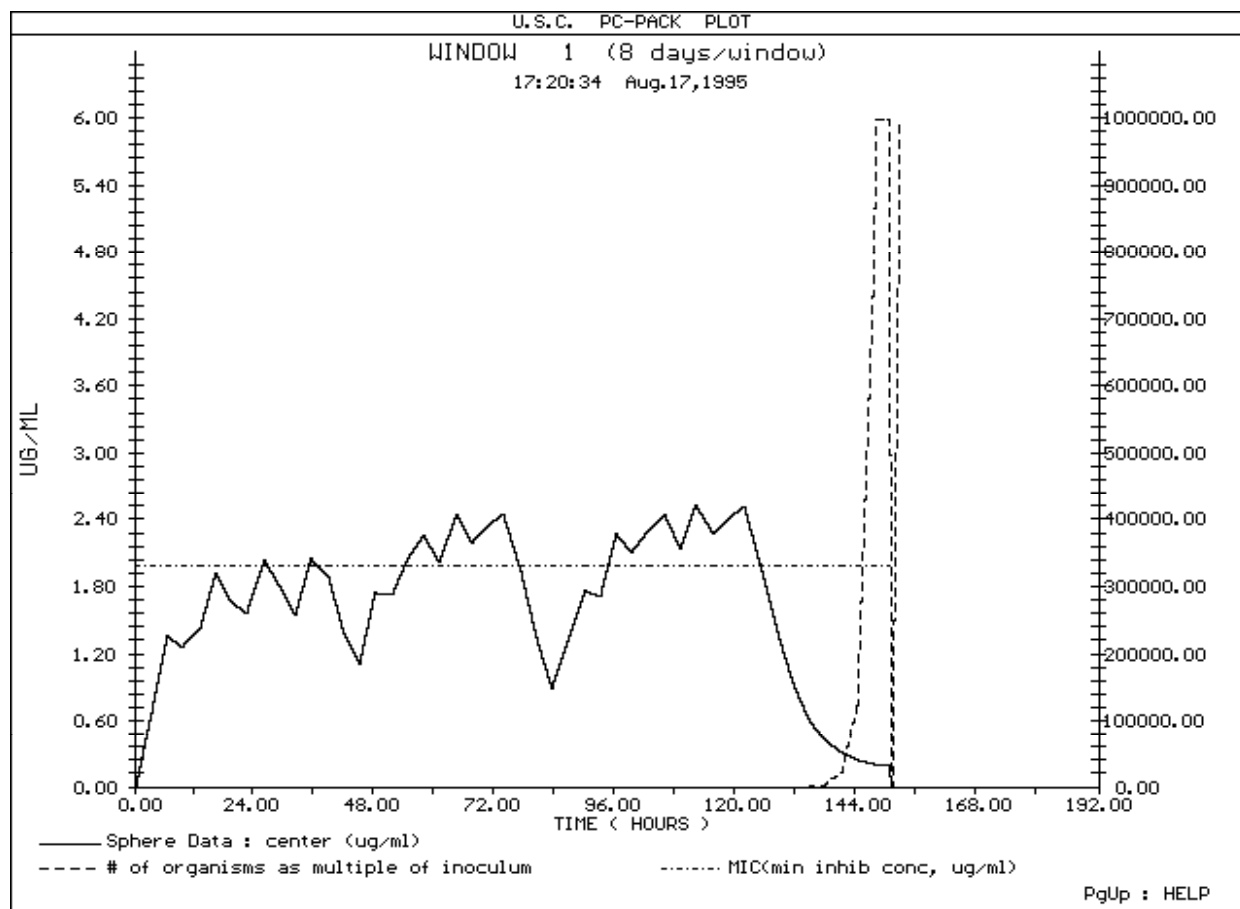


Figure 15. Graph of effects found with the model simulating the PAE of about 6 hours. Solid line and left hand scale: drug concentrations in the microorganism simulating the post-antibiotic effect. Dashed line and right hand scale: relative numbers of organisms. The plot always begins with 1.0 relative units of organism, as shown on the right hand scale. Horizontal dashed line: the patient's MIC of 2.0 ug/ml.

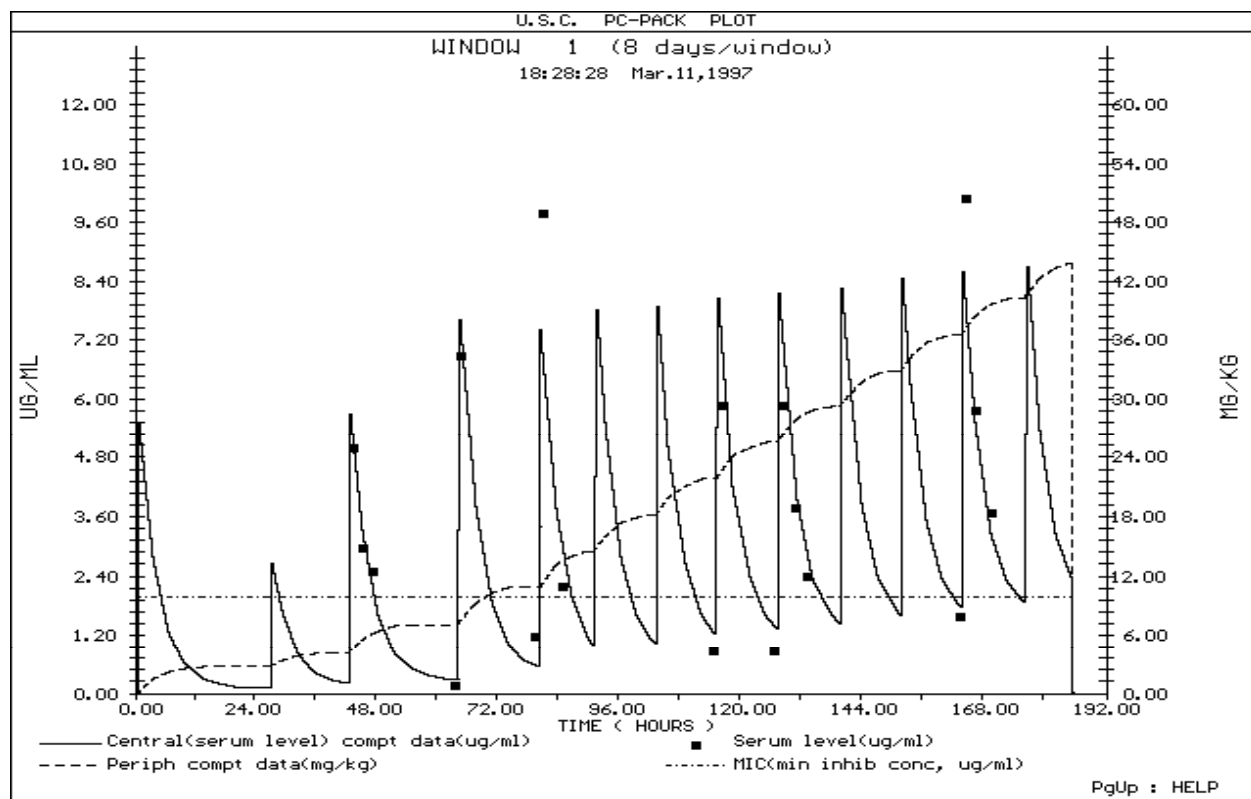


Figure 16. Plot of serum and peripheral compartment concentrations during the time of the patient's sepsis and his recovery. Small solid rectangles - measured serum concentrations. Solid line and left hand scale - fitted serum concentrations. Dashed line and right hand scale - peripheral compartment concentrations, also fitted from the serum data. Horizontal dashed line: the patient's MIC of 2.0 ug/ml.

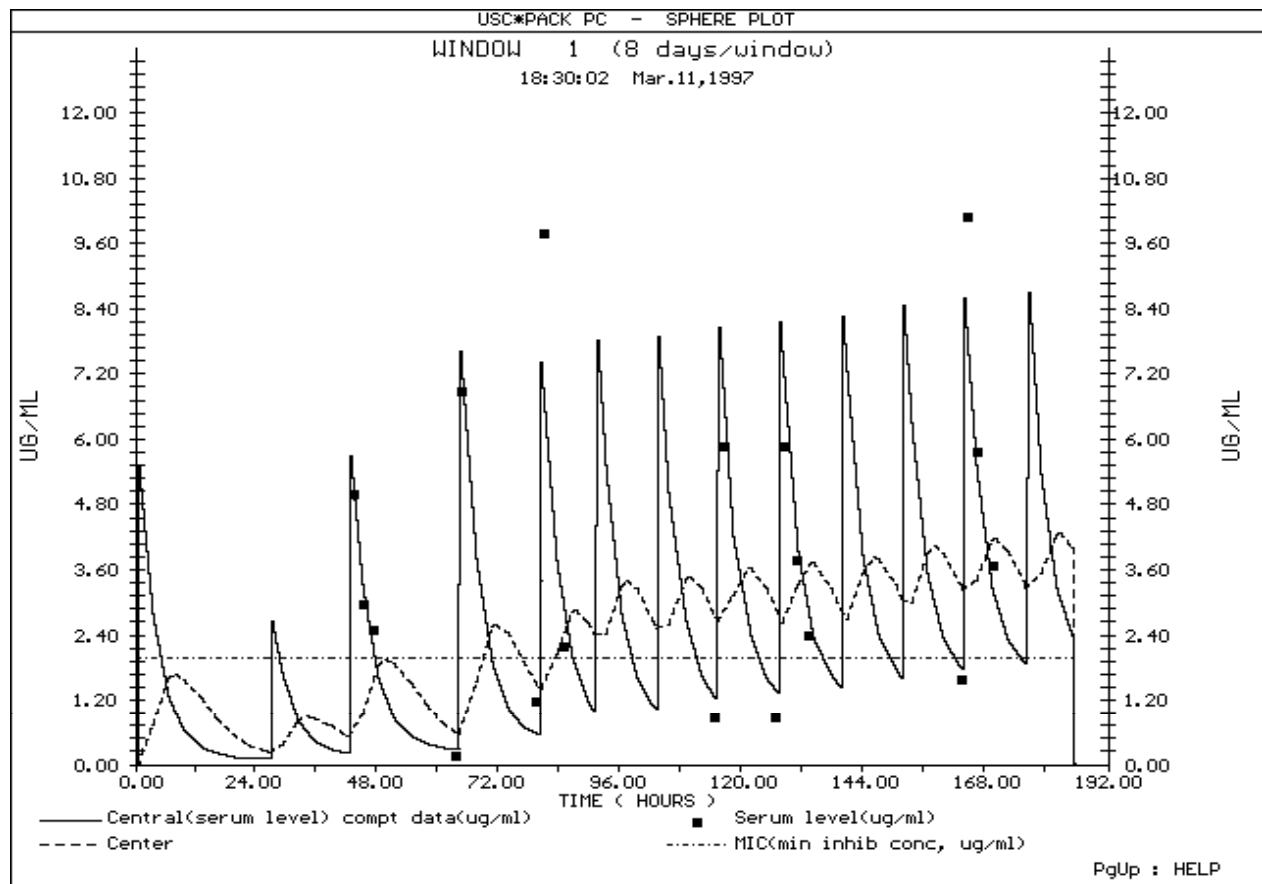


Figure 17. Plot of serum concentrations and computed concentrations in the center of the simulated microorganism simulating a 6-hour post-antibiotic effect. Small solid rectangles - measured serum concentrations. Solid line and left hand scale - fitted serum concentrations. Dashed line and right hand scale - computed concentrations in center of simulated microorganism. Horizontal dashed line: the patient's MIC of 2.0 ug/ml.

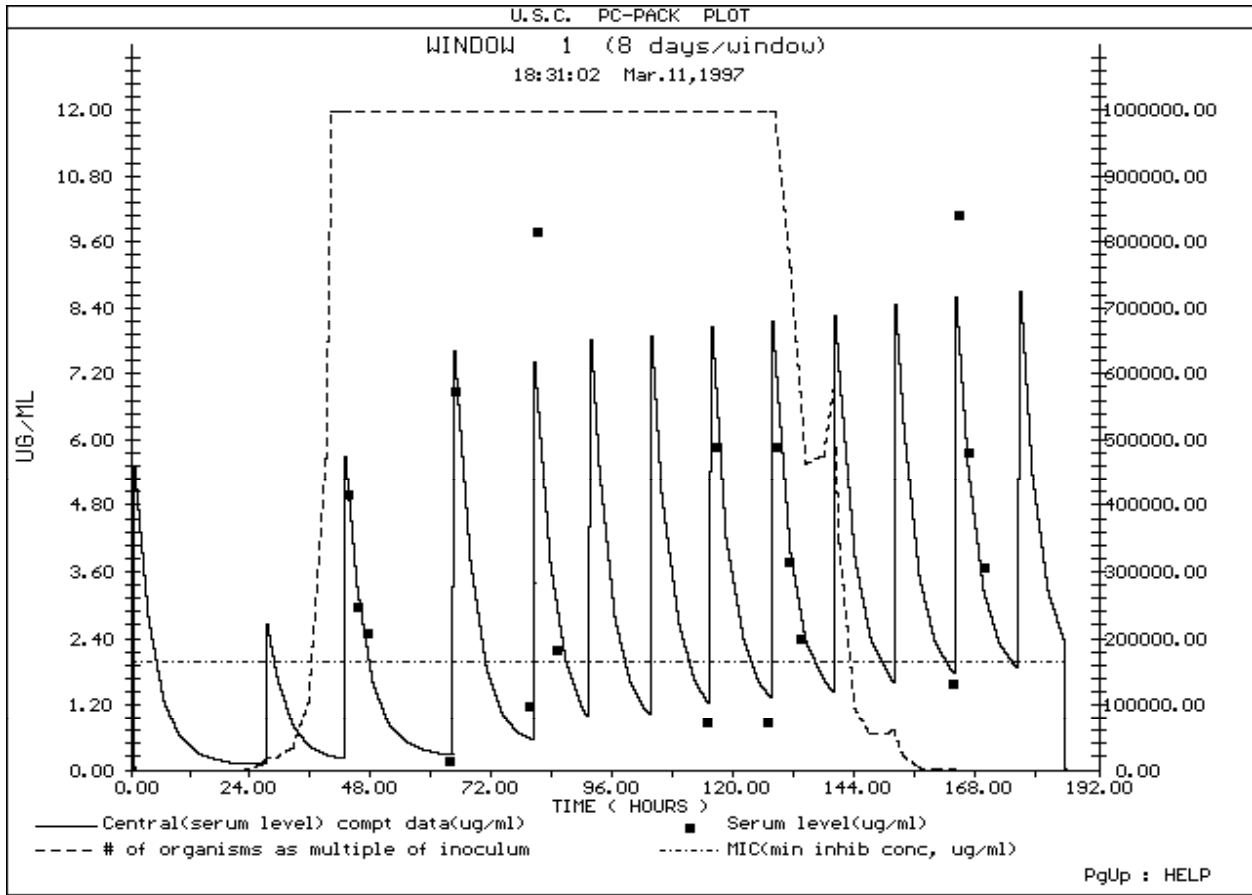


Figure 18. Plot of the effect on growth and kill using input from the serum concentration profile. The organisms grow out of control when serum concentrations are lower, but kill again when they are higher. These events correlated well with the patient's relapse at the beginning of the plot, and his recovery about one week later. Small solid rectangles - measured serum concentrations. Solid line and left hand scale - serum concentrations. Dashed line and right hand scale - relative numbers of organisms, with 1.0 relative unit present at the start of therapy. Horizontal dashed line: the patient's MIC of 2.0 ug/ml.



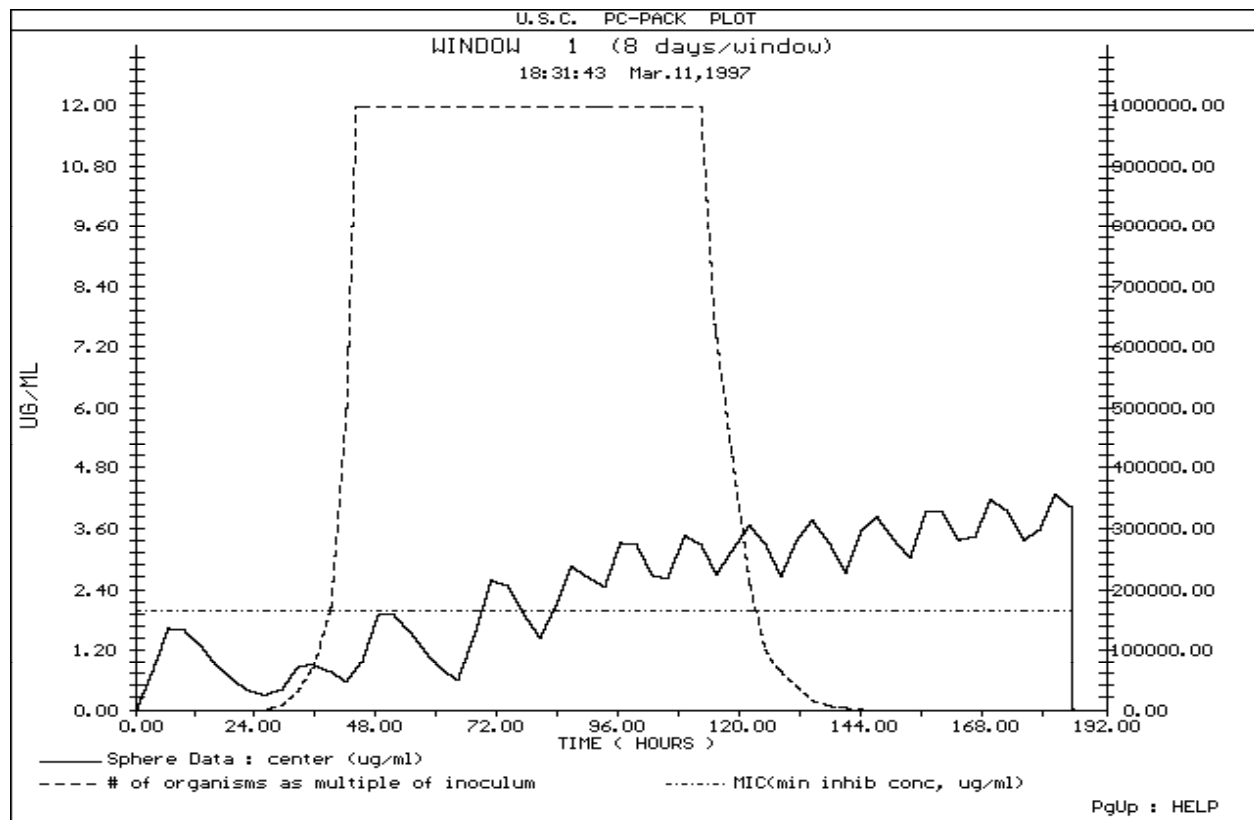


Figure 19. Plot of the effect on growth and kill using input from the center of the organism, using its computed concentrations as input to the effect model. The post-antibiotic effect helps somewhat to delay the relapse and to augment the kill. Solid line and left hand scale - computed concentrations in center of microorganism simulating the post-antibiotic effect. Dashed line and right hand scale - relative numbers of organisms, with 1.0 relative unit present at the start of therapy. Horizontal dashed line: the patient's MIC of 2.0 ug/ml.